공학석사 학위논문

OpenFOAM을 이용한 계류 시스템의 동적 해석 프로그램 개발

Development of dynamic analysis program for a mooring system using OpenFOAM

지도교수 이 승 재

2019년 8월

한국해양대학교 대학원

조선해양시스템공학과

서 유 정

본 논문을 서유정의 공학석사 학위논문으로 인준함.

위원장 이 성 욱 (인)

위 원 이 승 재 (인)

위 원 조 효 제 (인)

2019년 06월 21일

한국해양대학교 대학원

Table of contents

List of Tables

List of Figures

Development of dynamic analysis program for a mooring system using OpenFOAM

Yu Jeong Seo

Department of Naval Architecture and Ocean Systems Engineering
Graduate School of Korea Maritime and Ocean University

Abstract

부유식 해상 구조물은 작업 중 위치 유지 시스템을 위해서 계류선을 사용한다. 계류 시스템을 사용하는 부유식 구조물의 경우에는 정확한 구조물의 거동 해석을 위해서 계류선의 영향이 고려되어야 한다. 계류선의 운동은 비선형성을 띄기 때문에, 시간에 따른 계류선의 형상, 장력을 현수선(catenary) 계류선으로 표현하기에 한계가 존재한다. 본 연구에서는 계류선의 동적 해석을 수행하기 위하여 집중 질량법(lumped mass method)을 사용하여 계류선을 설계하였다. 하나의 계류선은 여러 개의 질점과 무게가 거의 없는 탄성력을 가진 스프링으로 구성되어 있으며, 이 단계에서는 질점의 부가 질량과 항력으로 인한 감쇠력의 영향은 고려되지 않는다. 설계된 계류선이 연결된 부유식 구조물의 운동을 해석하기 위해서 점성의 효과를 고려하는 전산 유체 역학(Computational Fluid Dynamics) 해석 방법을 사용하였다. 계류 시스템의 해석 프로그램은 C++ 라이브러리 기반의 오픈 소스 프로그램인 OpenFOAM과 연결되어 부유식 구조물과 계류 시스템의 커플링(coupling) 해석을 수행하였다. 계류선이 연결된 부유식 구

조물의 운동 응답 해석을 진행하였고, 수치해석 결과를 상용 계류 해석 프로그램인 Orcaflex 결과와 참조한 Quasi-static 해석결과 그리고 실험 결과와 비교 및 분석하였다.

KEY WORDS: Hydrodynamics 유체동역학, Mooring system 계류 시스템, Lumped mass method 집중 질량법, Dynamic analysis 동적 해석, Computational Fluid Dynamics 전산 유체 역학, OpenFOAM 오픈폼

Chapter 1. Introduction

1.1 Background

Floating offshore structure is important in terms of motion response in operating condition and seakeeping performance. In this study, the mooring system was used to maintain the location of the offshore structure in the wave. Because of the effect of the mooring system, the motion of the offshore structure keeps changing. The mooring line is often designed using the catenary equation, which is not able to analyze a change of shape and force of the mooring line over time. Since a motion of the mooring line is nonlinear, it is difficult to analyze the motion of the mooring line accurately with the catenary equation. In order to calculate the effect of the mooring line on the offshore structure, the mooring line should be designed to be able to consider changes of shape and force of the mooring line over time. For analysis of the mooring dynamic, we used the mooring line modeled by lumped-mass method which replaces the mooring line with lumped-mass and weightless springs.

Potential-based numerical technique is used to analyze the floating offshore structure and mooring system. While the potential-based analysis has an advantage of shorter simulation time because it does not take viscosity into account, the motion of offshore structure caused by effect of viscosity can not be analyzed. In order to solve this issue, Computational Fluid Dynamics (CFD) is used considering the effect of viscosity. In this study, CFD is used to analyze the global performance of a hull-mooring coupled system.

In order to analyze the mooring system, the catenary equation and lumped mass methods may be used. The catenary equation is used to solve the catenary equation for a shape of mooring lines and line tensions at each time step. This method is not able to analyze the mooring dynamics. The lumped mass method is used analyze the mooring system by replacing the mooring line with the springs and the lumped mass. This method is able to analyze the mooring dynamics because the motion of each lumped mass is analyzed every time step.

1.2 Literature Review

The lumped-mass method has been used for modeling the mooring line. Huang(1994) developed a three-dimensional finite difference model integrating the axial elasticity of the cable and Khan and Ansari (1986) developed the lumped-mass method in three dimensions. The lumped-mass method has been extended to integrate bending and torsional elasticity of the cable segment using the finite-element analysis (FEA) approach (Garrett, 1982). The experiment that the chain was submerged into the water basin and the fairlead was excited by the sinusoidal horizontal motion was performed without a structure for the validation of the mooring lines designed using the lumped-mass method (Azcona et al., 2017). The mooring lines designed by the FEM method and lumped mass are compared each other (Paredes et al. ,2018).

An external mooring line code is connected to the CFD for global performance analysis. The mooring code conducts the quasi-static analysis or the dynamic analysis of the mooring line. If the mooring line code is designed using a catenary mooring, the quasi-static analysis is performed not considering the mooring dynamic. Choi and Lee (2017) developed the quasi-static analysis program for a catenary mooring system using OpenFOAM and compared the result of numerical analysis and simulation in the regular wave condition. Lee et al. (2018) conducted floating body motion analysis using OpenFOAM that is connected with the external mooring line code modeled by lumped-mass method named MoorDyn. The free decay test is performed, and the results of numerical analysis and simulation are compared. Wu et al. (2016) developed in-house mooring system module and conducted numerical analysis for the motion characteristics of floating body and mooring system through coupling with the commercial program, star ccm+.

The results of dynamic analysis of the mooring system are compared with the experimental results (Palm et al., 2016). Hall and Goupee (2015) designed a mooring line using the lumped mass method and this mooring line was coupled with FAST simulator which is the floating wind turbine simulator. In the regular wave condition, comparison of the results in terms of motion and tension from the simulation and experiment was conducted.

1.3 Objectives and scopes

In this study, we developed dynamic analysis library of a designed mooring system with lumped mass method. This library is connected with OpenFOAM (Open Field Operation and Manipulation), an open source CFD program based on C++, which allows two-way coupling analysis between structure and mooring lines. The effects of added mass and hydrodynamic damping are not considered at this stage. In order to compare and validate the developed modules, numerical analysis is conducted using Orcaflex which is a proven commercial mooring analysis program. And the quasi-static analysis and the experimental results (Choi, (2017)) are also compared.

Chapter 2. Development of dynamic analysis program

2.1 Governing equation for fluid domain

The fluid in the flow field is assumed to be incompressible, viscosity fluid. The continuity equation and the Navier-Stokes equation are used to calculate the velocity and pressure for the fluid in the flow field. Each equation is shown in Equation (1) and (2).

$$\frac{\partial \rho_m}{\rho t} + \nabla \cdot (\rho_m u_m) = 0 \tag{1}$$

$$\frac{\partial \rho_m u}{\partial t} + \nabla \cdot (\rho_m u_m u_m) - \mu_m \nabla^2 u_m = -\nabla p + \rho g \tag{2}$$

where ρ is the density, u is the fluid velocity in the flow field, t is the time, p is the pressure, μ is the viscosity coefficient, g is the gravitational acceleration, and subscript m is the physical property of the fluid mixed with water and air.

In order to express the free surface, we used the VOF method to distinguish the two types of fluid using the volume ratio α in a mesh. When a mesh is completely filled with water α is 1 and when a mesh is completely filled with air, α is 0. In the case of water surface, α is indicated by $0<\alpha<1$. The ratio of the density and viscosity of the two types of fluid is given by Equation (3), (4).

$$\rho(\alpha) = \rho_w \alpha + \rho_a (1 - \alpha) \tag{3}$$

$$\mu(\alpha) = \mu_w \alpha + \mu_a (1 - \alpha) \tag{4}$$

where subscripts a and w mean air and water, respectively. The change of α for calculating water surface is the same as the transport equation shown in Equation (5).

$$\frac{\partial \rho_m u}{\partial t} + \nabla \cdot (\rho_m u_m u_m) - \mu_m \nabla^2 u_m = - \nabla p + \rho g \tag{5}$$

2.2 Equation of motion

The equation of 6-degree of freedom motions of a floating body assumed as a rigid body is shown in Equation (6) and (7).

$$(F_{CG})_i = m\frac{d^2(x_{CG})_i}{dt^2} = m\ddot{x}_{CG} \tag{6}$$

$$(M_{CG})_i = \frac{d}{dt}(I_{ij}\frac{d(\theta_{CG})_i}{dt}) = I_{ij}\ddot{\theta}_{CG} \tag{7}$$

Equation (6) is the translational equation for the x, y, z direction and Equation (7) is rotational equation for the x, y, z axes. m and I_{ij} are the mass and moment of inertia of the floating body, $\ddot{x}_{CG}$ and $\ddot{\theta}_{CG}$ are the change of the acceleration elements, x_{CG} and θ_{CG} are the displacement of the translational and rotational motion of the floating body, F_{CG} and M_{CG} are the force from the translational motion and the moment from the rotational motion acting on the center of gravity of the floating body. F_{CG} and M_{CG} consist of the sum of three components as in Equation (8) and (9).

$$F_{CG} = F_S + F_D + F_M \tag{8}$$

$$M_{CG} = M_S + M_D + M_M \tag{9}$$

In terms of translational motion, F_S is the hydrostatic force, F_D is the hydrodynamic force, and F_M is the mooring line force.

2.3 Coupling algorithm between floating body and mooring lines

The incident wave is a regular wave and the mooring system designed using a lumped mass method is applied to maintain the position of the floating body. In the time domain, the fairlead coordinates according to the behavior of the body in the wave are input to the mooring system library. Then, the motion analysis of the mooring lines is conducted based on the fairlead coordinates and the tension of the mooring lines becomes the output value of the mooring system library. Fig.1 shows a diagram of coupled analysis according to the correlation between incident wave, floating body and mooring system.

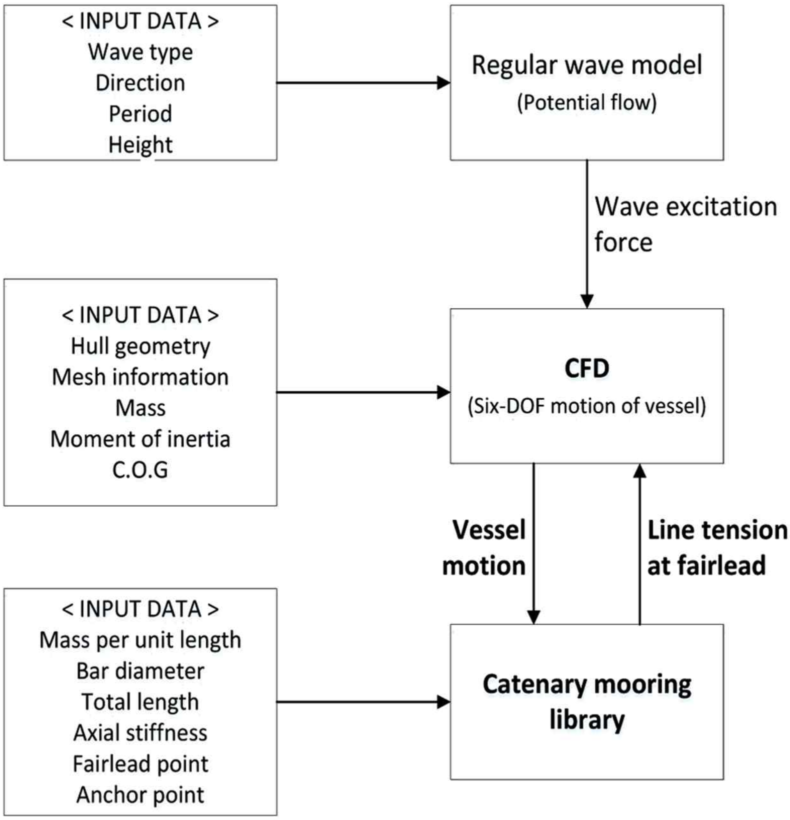

Fig.1 Coupled analysis diagram

2.4 Analysis algorithm

The VOF transport equation and the governing equation of fluid are discretized by Finite Volume Method. The time term in the governing equation is the Euler scheme of the first order accuracy, and the space term is the Linear upwind scheme of the second order accuracy. We use PIMPLE algorithm which combines SIMPLE algorithm and PISO algorithm for the relative velocity and pressure. The analysis process is shown in Fig.2.

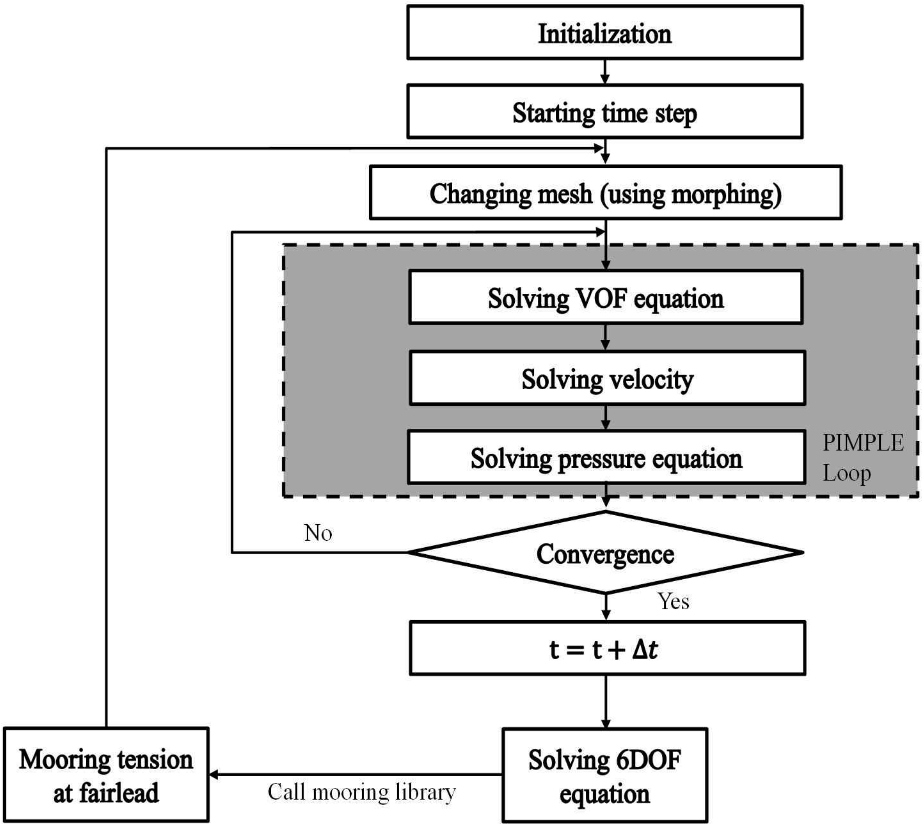

Fig.2 Flowchart of solving algorithm (Choi & Lee, 2017)

2.5 Principal particulars

Table 1 and Table 2 show the principal particular of the model ship and the mooring lines used to validate the developed dynamic analysis program, respectively. In order to reduce computation time, the barge-type model ship was used. Fig.3 shows the model ship in a full depth condition. The black line which is in the middle of the model ship is the draft. The model ship has no mother ship, but the scale factor is set to 300 considering the actual ship.

Table 1 The principal particular of the model ship

Description	Magnitude	Units
Length	0.8	m
Breadth	0.15	m
Depth	0.14	m
Draught	0.07805	m
Mass	9.366	kg
Vertical center of gravity	-0.04596	m
Vertical center of buoyancy	-0.03903	m
Moment of inertia around X-axis	0.011653	$kg \cdot m^2$
Moment of inertia around Y-axis	0.2406	$kg \cdot m^2$
Moment of inertia around Z-axis	0.24179	$kg \cdot m^2$

Table 2 The principal particular of the mooring lines

Description	Magnitude	Units
Line length	1.4	m
Line diameter	0.0018	m
Mass per unit length	0.12	kg/m
Submerged weight per length	0.1174	N/m
Elasticity (EA)	85400.0	N

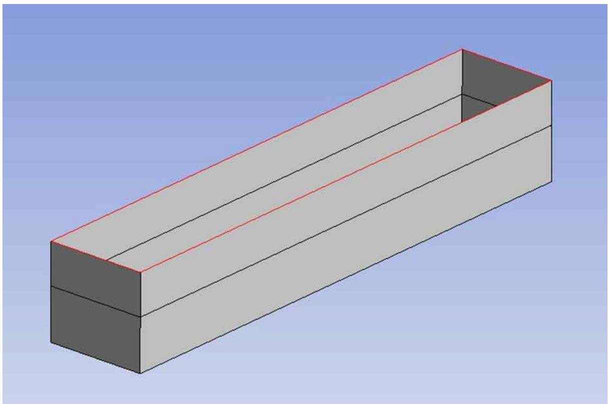

Fig.3 The model ship with full depth

2.6 Environmental condition

The computational domain is modeled as 25m(L)×1m(B)×1m(D). The floating body is located by one wavelength away from the boundary condition of the inlet. In order to minimize the wall effect, the relaxation zones are specified in the boundary conditions on the front, back, and both sides of the flow field. Considering that this study is a basic research, the maximum wave slope of the incident wave is less than 3 degrees to minimize the uncertainty. Table 3 shows the amplitude, direction, and period of the incident wave.

Table 3 Regular wave condition

Wave amplitude [m]	Wave direction [deg]	Wave period [s]
0.01	0.0	1.2, 1.4, 1.6, 1.8
0.03		

2.7 Mesh sensitivity test

Mesh sensitivity test was conducted with the regular wave prior to the analysis of floating motion responses in the wave. Fig.4 and Fig.5 were referred from Choi and Lee (2017). Fig.4 shows the magnitude of the wave amplitude according to the number of grids in the z-direction based on the wave that the period is 1s. The x-axis represents the number of grids in the direction of the wave amplitude, and the y-axis represents the measured wave amplitude.

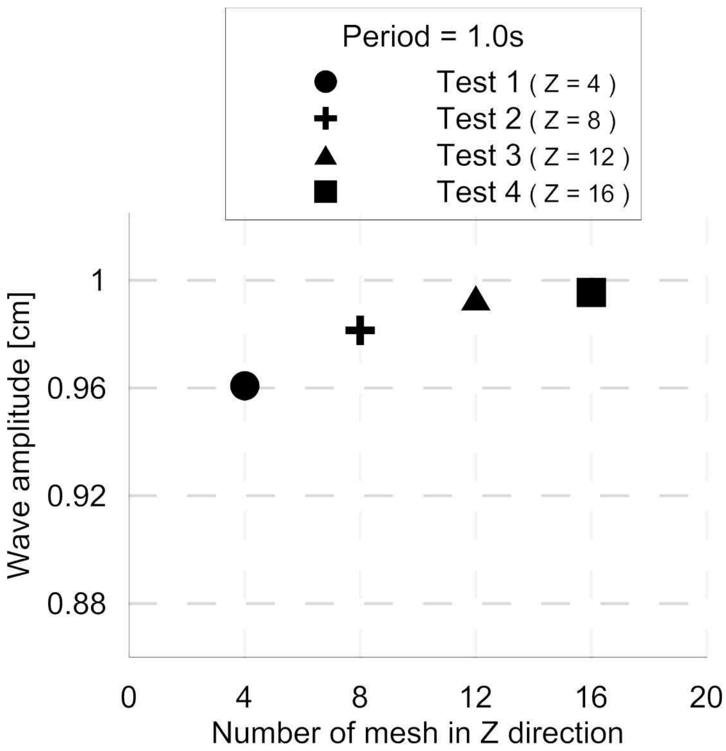

Fig.4 Mesh sensitivity test (Choi & Lee, 2017)

Comparing the input wave amplitude with the calculated wave amplitude, Test1 which has the largest mesh size had an error of about 4% and Test4 which has the smallest mesh size had an error of about 0.5%. Considering the accuracy and time of computation, the mesh size of Test3 with an error of approximately 0.7% was selected from the mesh sensitivity test.

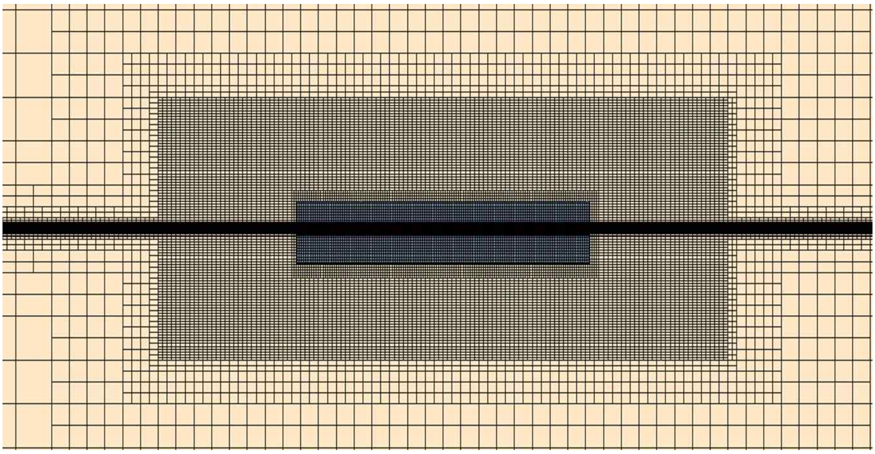

Fig.5 Computational mesh of domain (Choi & Lee, 2017)

Fig.5 indicates mesh distribution in the X-Z plane of flow field. For calculation of free water surface, the mesh in the region where the wave passes was fine, and about 130 grids in the X direction and 12 grids in the Z direction were used based on one wavelength. The mesh density around the floating body was increased. The total number of mesh used is 1.3 million.

Chapter 3. Dynamics of mooring lines

The process of calculating the mooring force consists of a static calculation and dynamic calculation stages. Fig.6 shows the two calculation stages briefly. The static calculation stage determines the shape of the mooring lines and pretensions. The dynamic calculation stage replaces the obtained mooring lines with the springs and lumps of mass and analyzes the motion of the mass.

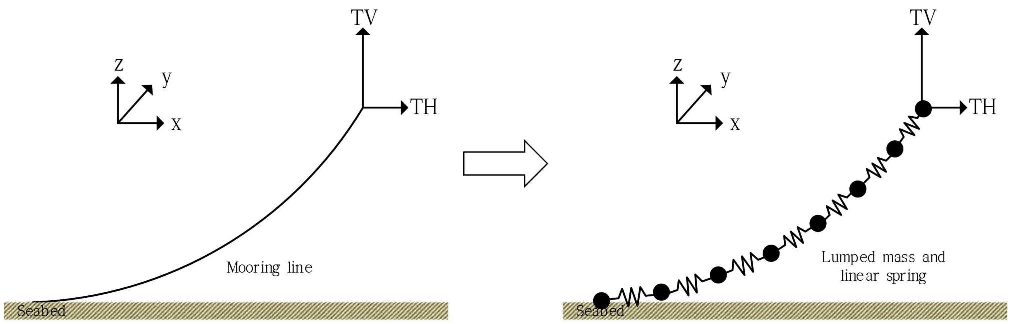

(a) The static calculation (b) The dynamic calculation

Fig.6 The two calculation stages

In this study, four mooring lines were connected to the port and starboard of the bow and starboard, respectively, and the mooring line lay-out is shown in FIg.7. The mooring lay-out is non-realistic. To reduce the uncertainty of the mooring system analysis code, one line per bundle was chosen.

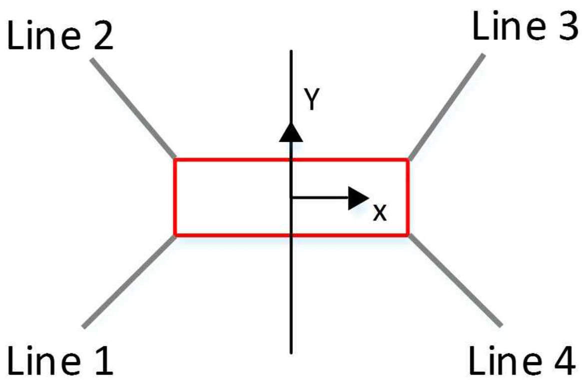

Fig.7 Mooring line lay-out

3.1 Static calculation

The shape of the mooring line was calculated using the catenary equation. The catenary equation used is shown in Equation (10), (11). This process is performed only once with the start of the motion analysis of the structure.

$$x(s) = \frac{TH}{w}\left[\sinh^{-1}\left(\frac{TV_a + w \bullet s}{TH}\right) - \sinh^{-1}\left(\frac{TV_a}{TH}\right)\right] + \frac{TH \bullet s}{K} \tag{10}$$

$$z(s) = \frac{TH}{w}\left\{\sqrt{1+\left(\frac{TV_a + w \bullet s}{TH}\right)^2} - \sqrt{1+\left(\frac{TV_a}{TH}\right)^2}\right\} + \frac{TV_a \bullet s}{K} + \frac{w \bullet s^2}{2K} \tag{11}$$

where s is the arc length of the mooring line from the sea floor to the fairlead, $x(s)$ and $z(s)$ are the displacement in the x and z directions along the line length from the seabed, TH and TV_a are the tension in the horizontal and vertical directions at the anchor point, w is the weight per unit length of the mooring line, and k is the axial stiffness of the mooring line.

3.2 Dynamic calculation

The mooring line was designed using the lumped mass method to analyze the mooring dynamic. One line consisted of several lumps of mass and elastic springs. At this stage, hydrodynamic damping and the effect of added mass was not considered. The input values are the coordinates of the fairlead and anchor and output value is the tension acting on the fairlead. From motion analysis program to mooring module, the information of coordinates of the fairlead and anchor is transferred. From mooring module to motion analysis program, the information of tension acting on fairlead is transferred.

At one time step, the fairlead tension is calculated by numerical analysis using the coordinates of fairlead, anchor, and lumped masses. As a method for numerical analysis of the motion of the lumped masses, the 4th Runge-Kutta method was used which has high accuracy. The spring force was calculated using the coordinates of the lumped mass and the neutral length of the spring. The restoring force of arbitrary spring is given by Equation (12).

$$f_i = k_i\left(\sqrt{(x_i - x_{i-1})^2 + (y_i - y_{i-1})^2 + (y_i - y_{i-1})^2} - l_i\right) \tag{12}$$

where f is the restoring force of the spring, k is the stiffness of spring, x, y, and z are the coordinates in x, y, z direction of the lumped masses, and l is the neutral length of the spring. The direction vector of the lumped masses is given by Equation (13).

$$\vec{r} = (x_i - x_{i-1})i + (y_i - y_{y-1})j + (z_i - z_{i-1})k \tag{13}$$

The motion equation of the mooring line is shown in Equation (14).

$$m_i \ddot{\vec{r}} + c_i \dot{\vec{r}} = f_{i-1} \frac{\overrightarrow{r_{i-1}}}{\left|\overrightarrow{r_{i-1}}\right|} - f_i \frac{\vec{r_i}}{\left|\vec{r_i}\right|} \tag{14}$$

where m is the mass of a lumped mass, c is the damping coefficient, g is the gravitational acceleration, $\dot{\vec{r}}$ is the velocity vector of the lumped mass, $\ddot{\vec{r}}$ is the acceleration vector of the lumped mass. Fig.8 shows a diagram of the force acting on the lumped mass.

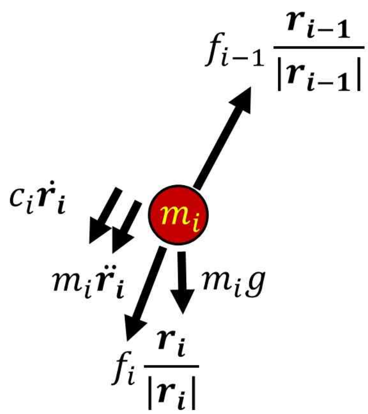

Fig.8 Force diagram acting on a lumped mass

The spring slack condition is considered by disabling the spring force as Equation (14). The slack condition is when the length of the spring becomes shorter than the neutral length of the spring.

$$f_i = k_i\left(\sqrt{(x_i - x_{i-1})^2 + (y_i - y_{i-1})^2 + (y_i - y_{i-1})^2} - l_i\right) = 0 \tag{14}$$

where *f* is the restoring force of the spring, *k* is the stiffness of the spring, *x, y,* and *z* are the coordinates of the lumped masses in x, y, z directions, and *l* is the neutral length of the spring.

The mooring lines have a touchdown zone. Since the seabed was not designed, a different method is applied. If the z-coordinate of the lumped mass becomes lower than the depth of water during the motion analysis, the process of adjusting the coordinates to the depth of water is performed at every time step.

Chapter 4. Numerical analysis results

Dynamic analysis results is compared with Orcaflex, Quasi-static analysis (Choi, (2017)), and Experiment results (Choi, (2017)). The quasi-static analysis used a catenary mooring system and Experiment was conducted at two-dimensional wave basin in KMOU (Korea Maritime and Ocean University). The results of hull motion and line tension are compared.

4.1 Static results

After connecting the mooring line to the floating body, the profile of the mooring line and the tension acting on lumped masses were compared before applying the wave force. Fig.9 shows comparison of the profile of the Line 1 from OpenFOAM and Orcaflex after static calculation. Since dynamic analysis and Quasi-static analysis used the same catenary equation, only the results of dynamic analysis results were plotted. The horizontal and vertical axes indicate the x and z axes, respectively, and the coordinates of the Line 1 are shown. The result of OpenFOAM(Dynamic) shows the coordinates of the lumped mass. The comparison shows that the developed program provides good agreement with the result from the Orcaflex.

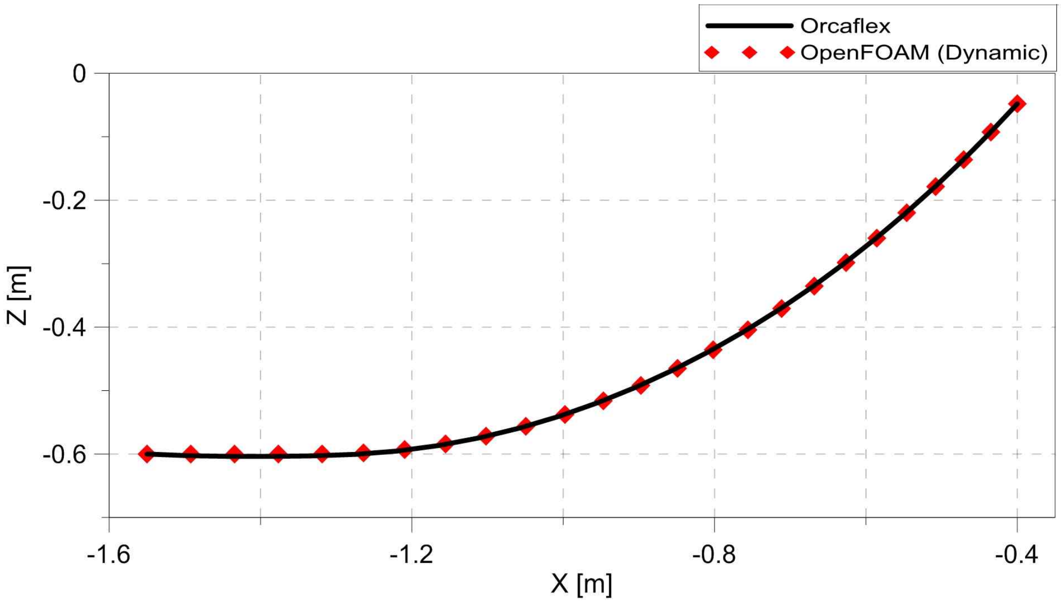

Fig.9 Profile of mooring line after static calculation

Fig.10 shows the comparison of the tension acting on the lumped masses of the Line 1 of the OpenFOAM and Orcaflex, which is calculated by restoring force of the springs. The horizontal axis represents a number of the lumped mass, and the vertical axis represents the effective tension. The number of the lumped mass is counted starting from the fairlead. For comparison, Orcaflex and OpenFOAM (Dynamic) had divided the Line 1 by the same number of segments. The difference between Orcaflex and OpenFOAM (Dynamic) is 0.2% to the minimum and 1.8% to the maximum and two results are in good agreement.

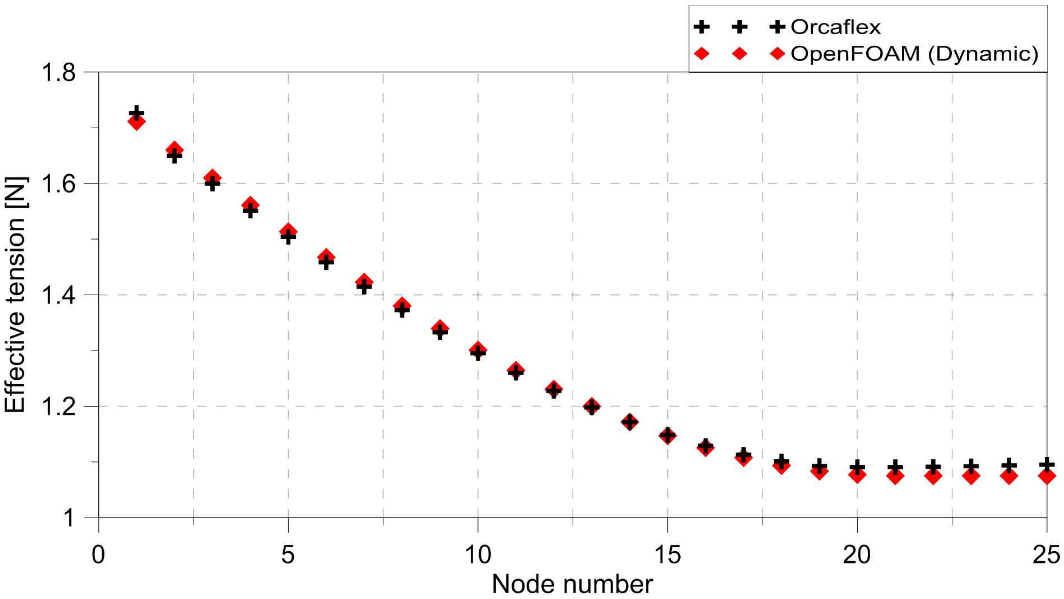

Fig.10 The tension acting on the lumped mass of Line 1

4.2 Behavior of floating body and mooring tension

The motion response of the floating body and the tension of the mooring lines were compared with the result of Orcaflex, Quasi-static analysis (Choi, (2017)), and Experiment results (Choi, (2017)) with respect to the period of incident regular wave under the head sea condition. The surge, heave, and pitch motion with the wave of 1.2s, 1.4s, 1.6s 1.8s period in two amplitudes were compared. Note that the results include the transient motinos in the initial stage and the phase is adjusted. Experimental data is raw data without any smoothing process so that the observed fluctuation is characteristics of experimental equipments.

The black line represents Orcaflex results, the red line represents dynamic analysis results using OpenFOAM, the blue line represents quasi-static analysis results using OpenFOAM, and the deep green line with rhombus represents experiment results.

Fig.11 to Fig 14 show the results of a regular wave test with an amplitude of 0.02m. Fig.11 shows time history of the surge, heave, and pitch motion response of the floating body with the wave of 1.2s period performed in Orcaflex, OpenFOAM (Dynamic), OpenFOAM (Quasi-static), and experiment. Fig.11 (b) and (c) show that all the results are qualitatively in good agreement. Fig.11 (a) shows that more low frequency components in OpenFOAM (Dynamic). Fig.12 shows time history of the motion response of the floating body with the wave of 1.4s period. Fig.13 shows time history of the motion response of the floating body with the wave of 1.6s period. Fig.14 shows time history of the motion response of the floating body with the wave of 1.8s period.

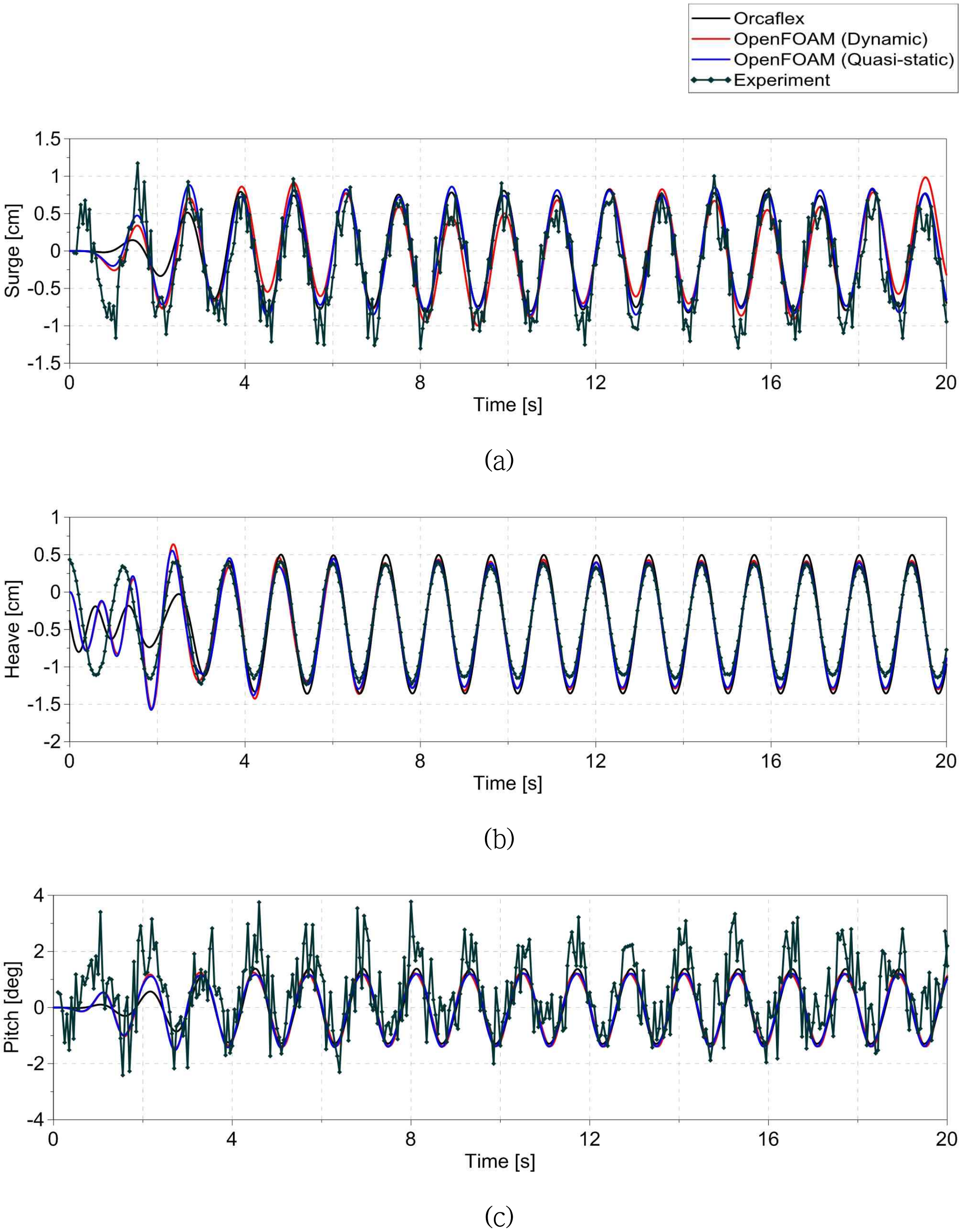

Fig.11 Time history of (a) Surge, (b) Heave, and (c) Pitch motion response (Period = 1.2s, Amplitude = 0.02m)

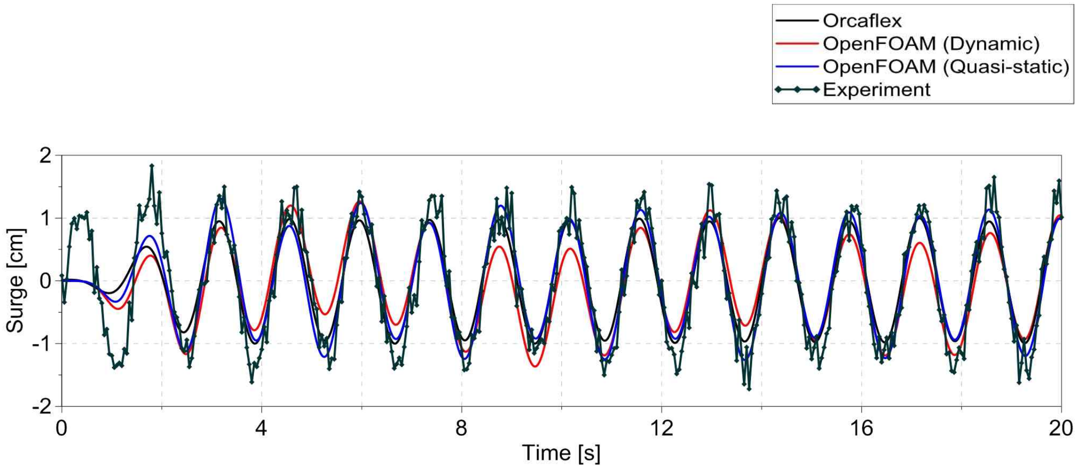

(a)

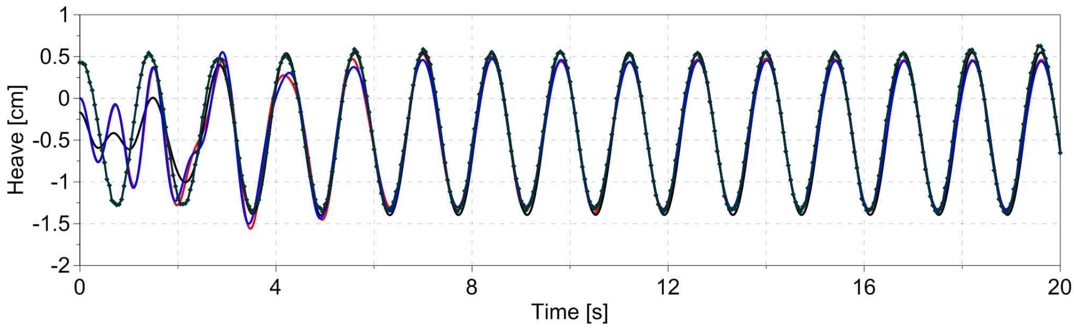

(b)

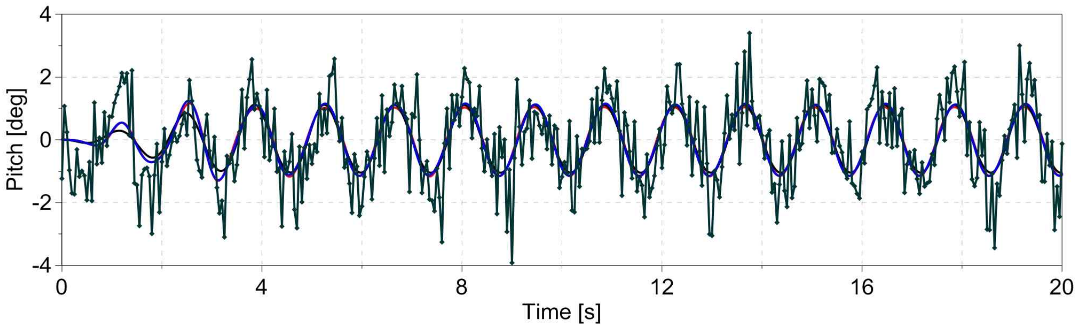

(c)

Fig.12 Time history of (a) Surge, (b) Heave, and (c) Pitch motion response (Period = 1.4s, Amplitude = 0.02m)

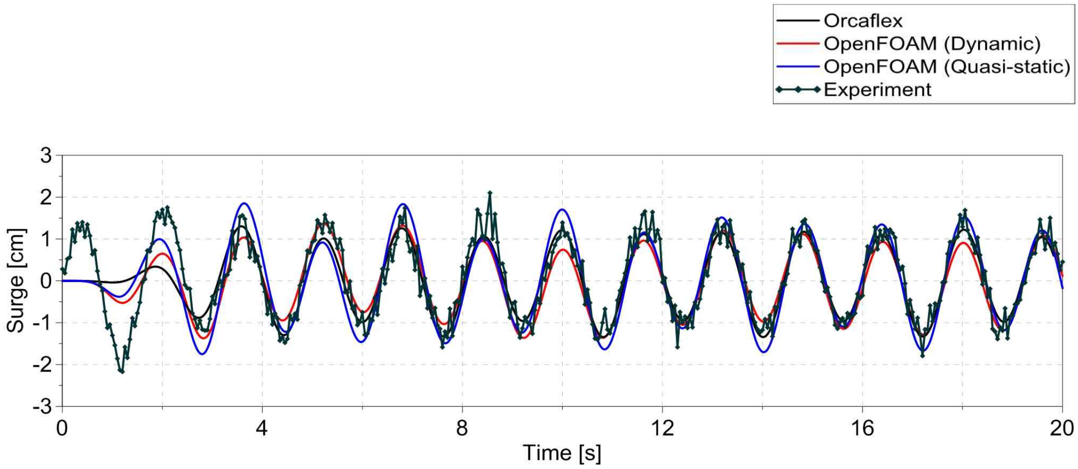

(a)

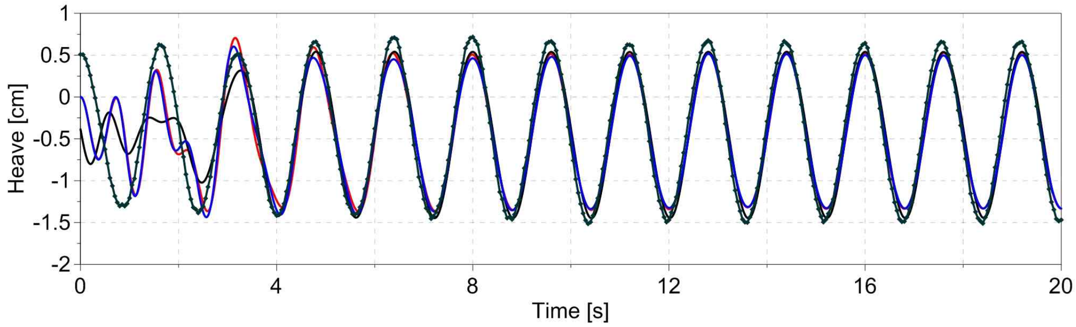

(b)

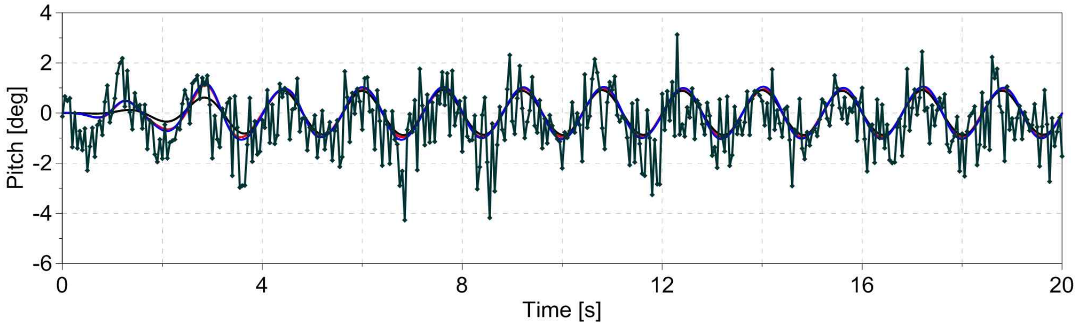

(c)

Fig.13 Time history of (a) Surge, (b) Heave, and (c) Pitch motion response (Period = 1.6s, Amplitude = 0.02m)

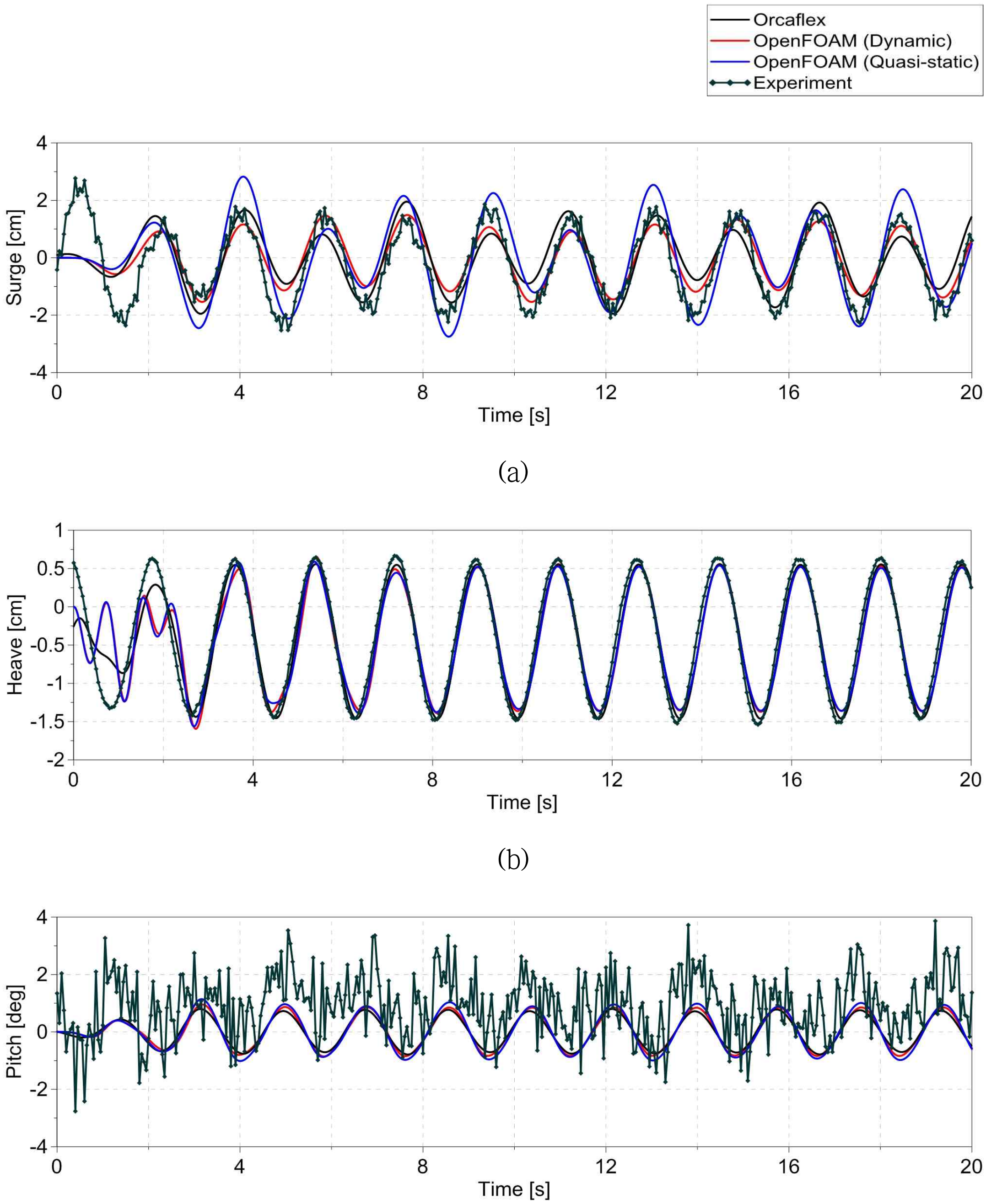

(a)

(b)

(c)

Fig.14 Time history of (a) Surge, (b) Heave, and (c) Pitch motion response (Period = 1.8s, Amplitude = 0.02m)

Fig.15 to Fig 18 show the results of a regular wave test with an amplitude of 0.06m. Fig.15 shows time history of the surge, heave, and pitch motion response of the floating body with the wave of 1.2s period performed in Orcaflex, OpenFOAM (Dynamic), OpenFOAM (Quasi-static), and experiment. Fig.15 (b) and (c) also show that all the results are qualitatively in good agreement. Fig.15 (a) shows that the OpenFOAM (Dynamic) has a magnitude about 1.4 times wider comparing with the other results and more low frequency components. Fig.16 shows time history of the motion response of the floating body with the wave of 1.4s period. Fig.16 (a) shows that OpenFOAM (Dynamic) has more low frequency components, but a magnitude is the same as results of the others. Fig.17 shows time history of the motion response of the floating body with the wave of 1.6s period. Fig.18 shows time history of the motion response of the floating body with the wave of 1.8s period.

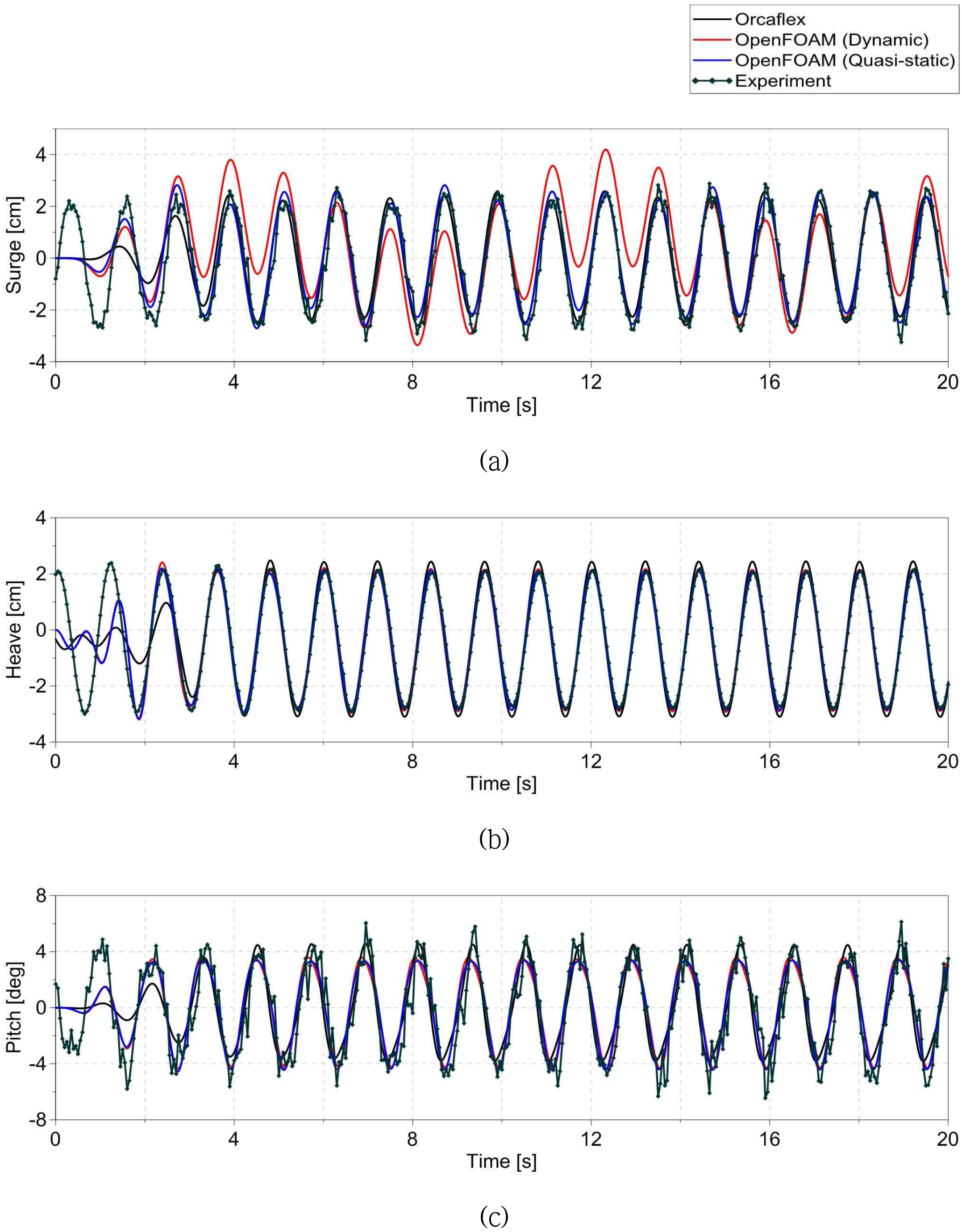

Fig.15 Time history of (a) Surge, (b) Heave, and (c) Pitch motion response (Period = 1.2s, Amplitude = 0.06m)

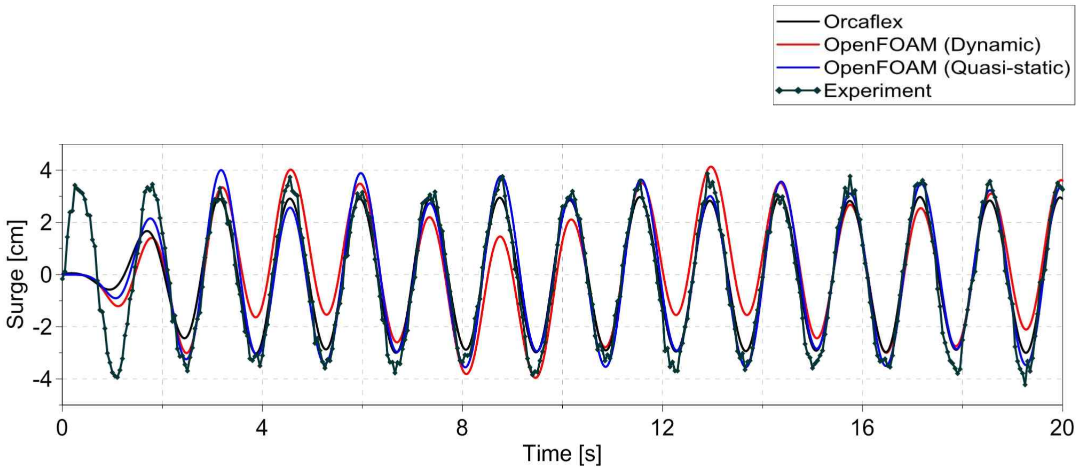

(a)

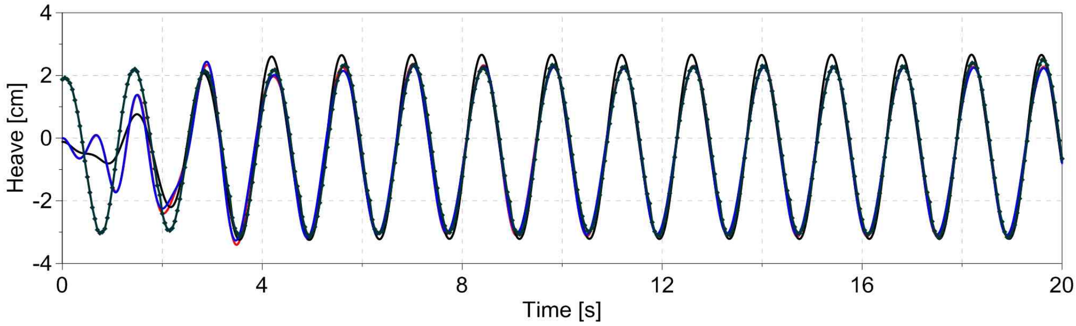

(b)

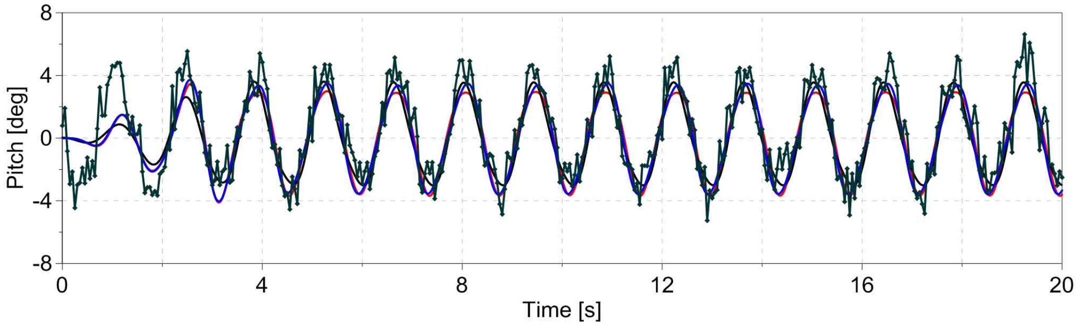

(c)

Fig.16 Time history of (a) Surge, (b) Heave, and (c) Pitch motion response (Period = 1.4s, Amplitude = 0.06m)

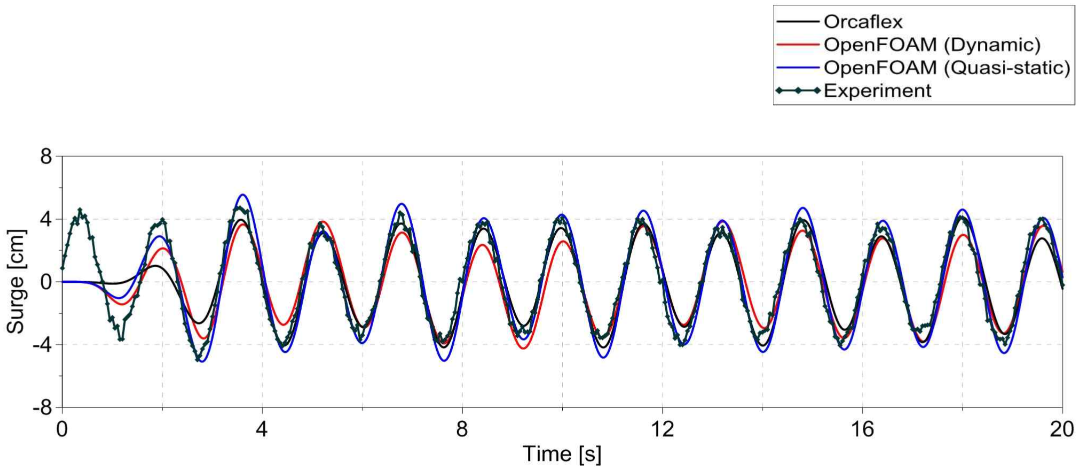

(a)

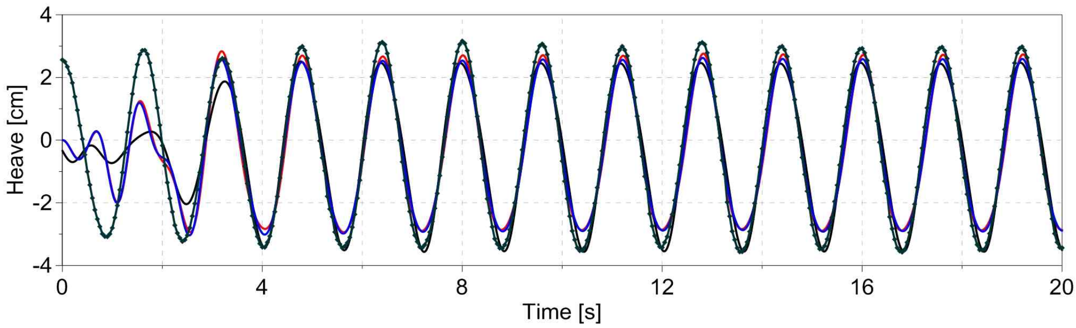

(b)

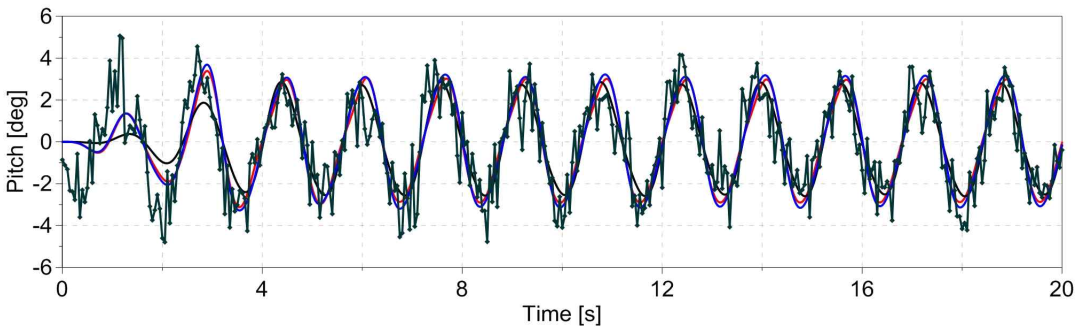

(c)

Fig.17 Time history of (a) Surge, (b) Heave, and (c) Pitch motion response (Period = 1.6s, Amplitude = 0.06m)

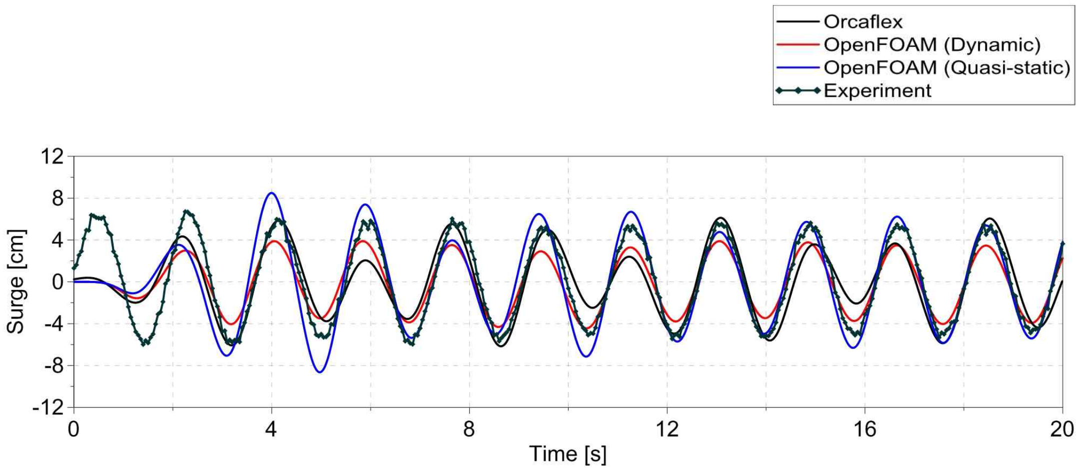

(a)

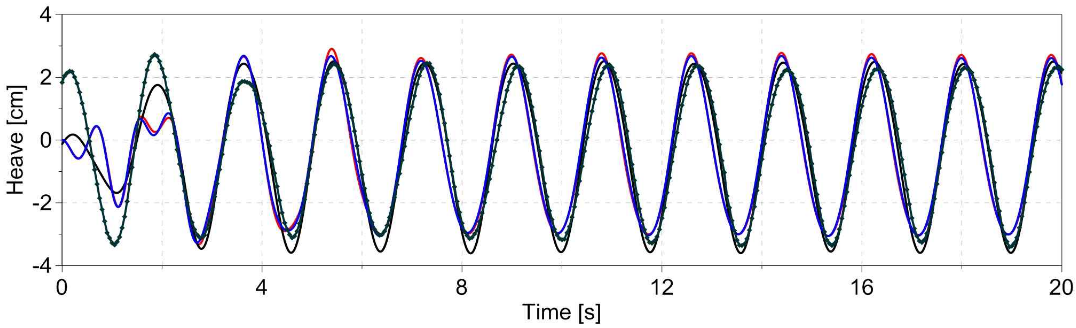

(b)

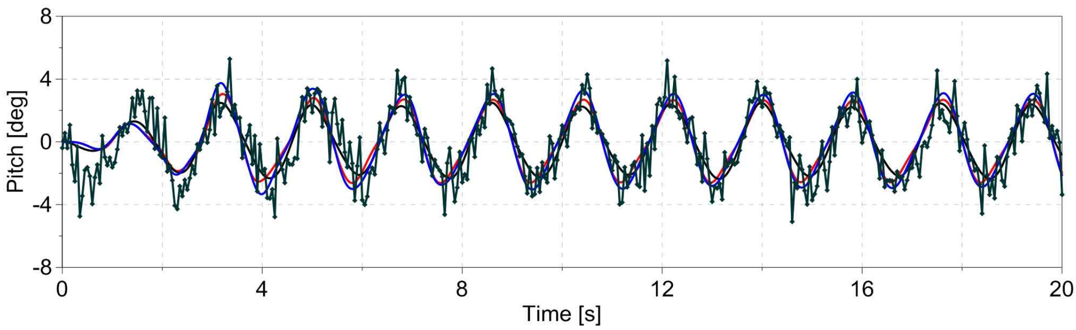

(c)

Fig.18 Time history of (a) Surge, (b) Heave, and (c) Pitch motion response (Period = 1.8s, Amplitude = 0.06m)

In all the results, the OpenFOAM (Dynamic) has resulted in different motions from the other three results in the surge motion, but has in a good agreement in heave and pitch motions. This motion is presumed to be related to the stiffness of the spring. When high stiffness of spring was used in the mooring code, the code became unstable. For better numerical stability in developed program, the softer spring with low axial stiffness was used in the code when replacing the mooring line with the spring and lumped mass. Characteristic of this modeling also affects the tension of the mooring lines.

Fig.19 shows the time history of mooring line tension at the fairlead (Period = 1.2s, Amplitude = 0.06m). Since the line configuration is symmetrical, it indicates the tension of Line1 and Line3 located on the diagonal from 10s to 20s. Fig.19 (a) shows that the period of tension of OpenFOAM (Dynamic) has about twice as different from the period of tension of Orcaflex and OpenFOAM (Quasi-static). The magnitudes of OpenFOAM (Quasi-static) and Orcaflex are about three times larger more than the magnitude of OpenFOAM (Dynamic). These results also shown in Fig.19 (b).

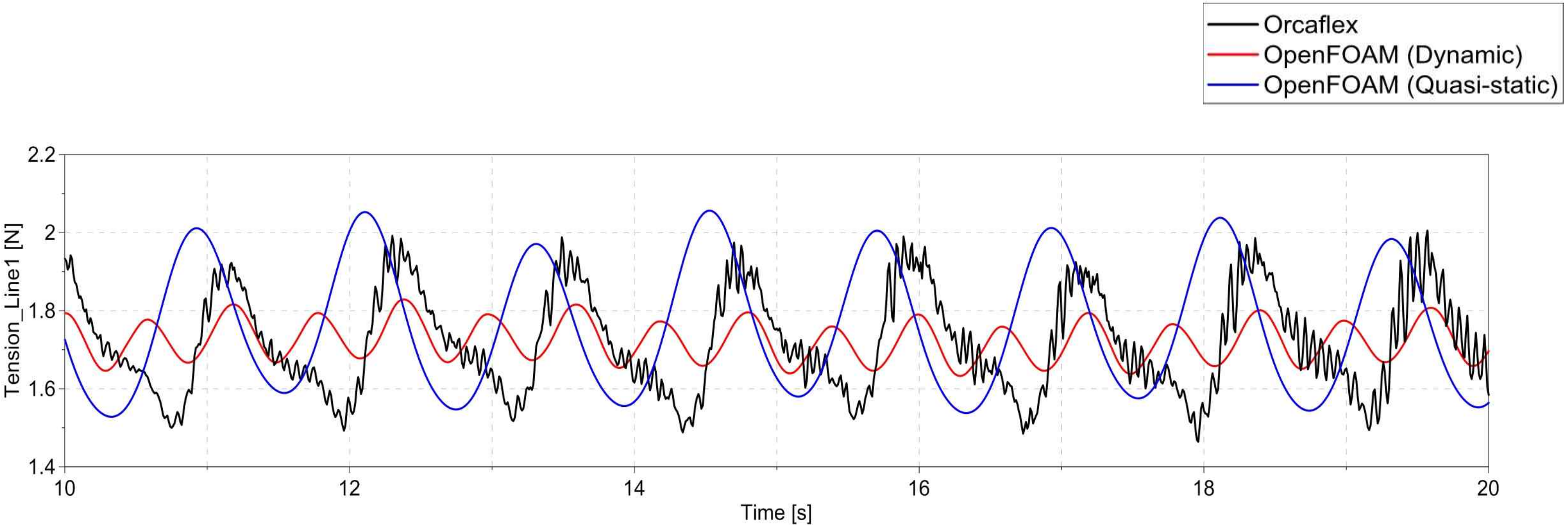
Orcaflex
OpenFOAM (Dynamic)
OpenFOAM (Quasi-static)
Tension_Line1 [N]
2.2
2
1.8
1.6
1.4
10
12
14
16
18
20
Time [s]

(a)

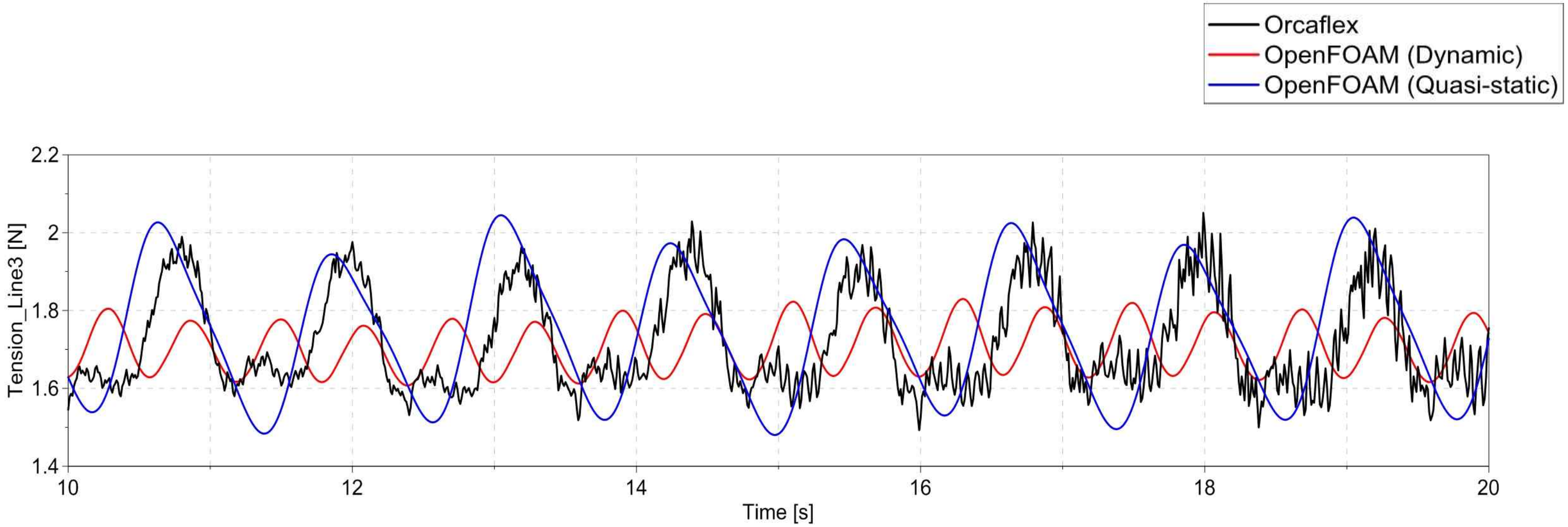

(b)

Fig.19 Time history of mooring line tension at fairlead (a) Line1 (b) Line3

(Period = 1.2s, Amplitude = 0.06m)

The results of developed dynamic analysis program include low frequency components compared with the results of Orcaflex, OpenFOAM (Quasi-static), and Experiment and have a good agreement in heave and pitch motions compared with the results of Orcaflex, OpenFOAM (Quasi-static), and Experiment. However, the results of the mooring tension of developed dynamic analysis program have a period that is twice the difference with the results of Orcaflex and OpenFOAM (Quasi-static). This is related to the moment of inertia due to the mooring lines. Since the moment of inertia around y-axis of the structure is four-times larger than the moment of inertia of the mooring lines, it does not have much effects on the behavior of the structure.

Chapter 5. Conclusion

In this study, the mooring system was modeled using the lumped mass method, and the coupling module of the floating body and the mooring dynamic system were developed using OpenFOAM, which is an open source CFD program. It was compared with the results of numerical analysis from the commercial program, Orcaflex. The shape and pretension of the mooring line were compared in the static equilibrium state. In the regular wave condition of the head sea condition, the motion response of the floating body and the pretension at the fairlead are qualitatively compared in the time domain. The following conclusions are drawn from this study:

First, the developed dynamic system program for a mooring system is confirmed to be in good agreement with Orcaflex in heave and pitch motions and shows more low frequency components. This phenomenon should be solved by increasing the stability of the code.

Second, the developed dynamic program have the different periods of the tension of the mooring lines compared with the other results.

Third, the developed program validates coupling effects on motion between the floating body and mooring system. In order to improve the accuracy and stability of the developed program, the mooring need to be refined.

Forth, the added mass and hydrodynamic damping force were not considered when designing the mooring line. The comparisons and validations are needed to account for these force in the future.

Fifth, numerical analysis was carried out without a mother ship in order to meet the performance of experimental equipment. Since this is a nonexistent specification, it is considered to be limited in realizing the physical phenomenon of the global performance.

Reference

최준혁, 2017. *OpenFOAM을 이용한 catenary 계류 시스템의 준정적 해석 프로그램 개발*. 석사학위논문. 부산:한국해양대학교.

Azcona, J., Munduate, X., González, L., & Nygaard, T. A. (2017). Experimental validation of a dynamic mooring lines code with tension and motion measurements of a submerged chain. Ocean Engineering, 129, 415-427.

Choi, J. H., and Lee, S. J. (2017). Development of Quasi-static Analysis Program for Catenary Mooring System using OpenFOAM. Journal of Ocean Engineering and Technology, 31(4), 274-280.

Huang, S. (1994). Dynamic analysis of three-dimensional marine cables. Ocean Engineering, 21(6), 587-605.

Garrett, D. L. (1982). Dynamic analysis of slender rods. Journal of energy resources technology, 104(4), 302-306.

Hall, M., & Goupee, A. (2015). Validation of a lumped-mass mooring line model with DeepCwind semisubmersible model test data. Ocean Engineering, 104, 590-603.

Khan, N. U., & Ansari, K. A. (1986). On the dynamics of a multicomponent mooring line. Computers & Structures, 22(3), 311-334.

Lee, S. C., Park, S., Song, S., & Jeong, S. M. (2018, July). Development of Platform 6-DOF Motion-Mooring System Coupled Solver Using Open Source Libraries. In The 28th International Ocean and Polar Engineering Conference. International Society of Offshore and Polar Engineers.

Paredes, G. M., Eskilsson, C., Palm, J., Kofoed, J. P., & Bergdahl, L. (2018, November). Coupled BEM/hp-FEM Modelling of Moored Floaters. In Vietnam Symposium on Advances in Offshore Engineering (pp. 504-510). Springer,

Singapore.
Palm, J., Eskilsson, C., Paredes, G. M., & Bergdahl, L. (2016). Coupled mooring analysis for floating wave energy converters using CFD: Formulation and validation. International Journal of Marine Energy, 16, 83-99.
Wu, G., Kim, J. W., Jang, H., & Baquet, A. (2016, June). CFD-Based Numerical Wave Basin for Global Performance Analysis. In ASME 2016 35th International Conference on Ocean, Offshore and Arctic Engineering (pp. V001T01A008-V001T01A008). American Society of Mechanical Engineers.